Songklanakarin J. Sci. Technol.
40 (5), 1081-1089, Sep. - Oct. 2018

http://www.sjst.psu.ac.th

Original Article

Co-combustion of rice husk pellets and moisturized rice husk in a fluidized-bed combustor using fuel staging at a conventional air supply

Pichet Ninduangdee[1*] and Vladimir I. Kuprianov[2]

[1] *Division of Mechanical Engineering, Faculty of Engineering and Industrial Technology, Phetchaburi Rajabhat University, Mueang, Phetchaburi, 76000 Thailand*

[2] *School of Manufacturing Systems and Mechanical Engineering, Sirindhorn International Institute of Technology, Thammasat University, Khlong Luang, Pathum Thani, 12121 Thailand*

Received: 31 July 2016; Revised: 27 June 2017; Accepted: 30 June 2017

Abstract

This paper presents an experimental study on co-combustion of two types of rice husk with substantially different properties in a fluidized-bed combustor using fuel staging for lowering NO emission. Rice husk pellets were burned as a base (or primary) fuel, whereas moisturized rice husk was injected downstream from the primary combustion zone as a secondary fuel. The experiments were conducted at 200 kW_{th} heat input to this reactor with a bottom air supply, while the energy fraction of the secondary fuel in the total heat input ranged from 0 to 0.25, and excess air was within 20–80% for each co-firing option. The study revealed significant effects of the operating parameters on combustion and emission performance of the combustor. Compared to burning of the base fuel, a nearly 40% NO emission reduction is achievable with fuel staging, while controlling the CO and C_xH_y emissions from the combustor to acceptable levels. However, fuel staging causes some deterioration in the combustion efficiency.

Keywords: fluidized bed, rice husk, co-combustion, fuel staging, NO reduction

1. Introduction

For many years, rice husk has been an important resource of bioenergy in Thailand. In 2014, some 8 million tons of rice husk were produced in this country, which is equivalent to 2,840 ktoe (or about 120 PJ) energy potential (Department of Alternative Energy Development and Efficiency [DEDE], 2014).

Due to its excellent combustion properties, rice husk has shown high potential and suitability as a fuel in the direct combustion systems at heat and power plants. A number of studies have reported high effectiveness of fluidized-bed combustion systems converting rice husk into energy (Fang *et al.*, 2004; Janvijitsakul & Kuprianov, 2008; Kuprianov *et al.*, 2010). When using conventional bed materials (silica/quartz sand), these systems are commonly free of the operational problem known as bed agglomeration (Duan *et al.*, 2013; Janvijitsakul & Kuprianov, 2008). This fact can be attributed to the favorable composition of rice husk ash (with a predominant content of Si and a rather low proportion of K), which prevents "coating-induced" and/or "melt-induced" bed agglomeration when burning rice husk (Visser *et al.*, 2008).

However, fluidized-bed combustion of rice husk is generally accompanied by elevated/ high NO_x emissions, whose level is dependent on fuel-N, operating conditions, and combustion method/technique used (Madhiyanon *et al.*, 2010; Sirisomboon *et al.*, 2010; Werther *et al.*, 2000). Having an insignificant fuel-N content, 0.2–0.5% (by wt., on an as-received basis), rice husk, nevertheless, can generate elevated and, in some cases, high NO_x emissions: up to 180 ppm (on a dry gas basis, and at 6% O_2) when fired in conventional fluidized-bed combustion systems (Chyang *et al.*, 2007; Fang

*Corresponding author
Email address: ninduangdee.p@gmail.com

et al., 2004; Kuprianov *et al.*, 2010), and up to 425 ppm when burning this biomass in fluidized-bed combustion systems with alternative hydrodynamics and/ or high combustion intensity (Madhiyanon *et al.*, 2004, 2006, 2010).

Co-firing of two or more fuels seems to be an effective technique to remedy this deficiency. The most important advantage of co-firing is its flexibility with regard to fuel type and combustion method, as established in studies on grate-firing, pulverized fuel-firing, and fluidized-bed combustion techniques (Areeprasert *et al.*, 2016; Nussbaumer, 2003; Sami *et al.*, 2001). A large number of studies have addressed various aspects of co-firing coal and biomass, commonly combusted as a blended feedstock in modified pulverized coal-fired boilers. In most co-firing tests on these boilers, a lowered net production of CO_2 and a substantial reduction in NO_x and SO_2 emissions have been achieved with a more stable combustion process and reduced costs of heat/ power generation compared to burning coal on its own (Narayanan & Natarajan, 2007; Sahu *et al.*, 2014; Sami *et al.*, 2001;).

However, not much information regarding biomass –biomass co-firing in fluidized-bed combustion systems is available in literature. The recent studies on (i) co-combustion of rice husk premixed with sugar cane bagasse and (ii) co-combustion of rubberwood sawdust blended with eucalyptus bark have revealed that problematic fuels (e.g., with rather low calorific value and/ or elevated emissions) can be effectively utilized by co-firing in a fluidized-bed combustor (Chakritthakul & Kuprianov, 2011; Kuprianov *et al.*, 2006). From these two studies, co-combustion of a biomass with a relatively high calorific value and a different one of higher fuel-moisture and/ or lower fuel-N can lead to a substantial reduction of NO_x emissions, whose level is dependent on the energy proportions of the blended fuels and on the amount of excess air.

Fuel staging has been proven an effective technique for reducing NO_x in a combustion system (co-) fired with coal/ biomass. In fuel-staged combustion, a base fuel is fed into the bottom region of the reactor together with combustion air and therefore fired with excess air. Meantime, the rest of the fuel (or a different fuel with dedicated properties) is delivered into the above zone with no air supply to create preferable conditions for NO_x reduction (Baukal, 2001). This technique can be readily applied in a co-firing system with the aim to ensure fuel staging (biasing) along the reactor height.

In a combination with the air-staged injection into a combustion system, the fuel staging can ensure a significant reduction in NO_x emissions, as shown in studies on the co-firing of two woody residues in a laboratory scale grate-fired system (Salzmann & Nussbaumer, 2001, 2003). Apparently, such a system requires a more complicated configuration of a furnace/ combustor (and so is more expensive) and a rather difficult control of primary air injection compared to that with a conventional (bottom) air supply. However, the literature sources lack information on biomass–biomass co-firing in fluidized-bed combustion systems using fuel staging (i.e., separate injection of primary and secondary fuels into a system) with a single-flow air injection through the air distributor fixed at the reactor bottom.

This work was therefore aimed at studying the effects of fuel staging (i.e., mass/ energy fraction of the co-fired fuels in the total heat input) and excess air on the combustion and emission performance of a fluidized-bed combustor co-fired with rice husk pellets and moisturized rice husk using a conventional (bottom) air injection system. An assessment of the NO emission reduction for specified operating parameters of the proposed combustor using fuel staging was the main focus of this work.

2. Materials and Methods

2.1 Experimental setup

Figure 1 shows a schematic diagram of the experimental setup with the cone-shaped fluidized-bed combustor (referred to as 'conical FBC') used in this work. The setup included the combustor (equipped with a nineteen bubble-cap air distributor) and auxiliary facilities, such as an air blower, two screw-type fuel feeders, a cyclone for collecting particulate matter, and a diesel-fired start up burner.

The conical FBC has been previously employed in studies on individual burning of some problematic biomass fuels, as reported by Ninduangdee and Kuprianov (2015 and 2016). However, compared to the previous configuration with a single fuel supply, the combustor was modified for the current study (equipped with an additional fuel feeder) to conduct co-firing tests for fuel staging. During the experiments, primary and secondary biomass fuels were delivered separately into the conical FBC by the two screw-type fuel feeders, as shown in Figure 1. The primary fuel was injected into the fluidized bed at 0.65 m level above the air distributor, whereas the secondary fuel was introduced into the cylindrical section 0.5 m higher, thus ensuring co-firing of the two biomass fuels using fuel staging with bottom air supply.

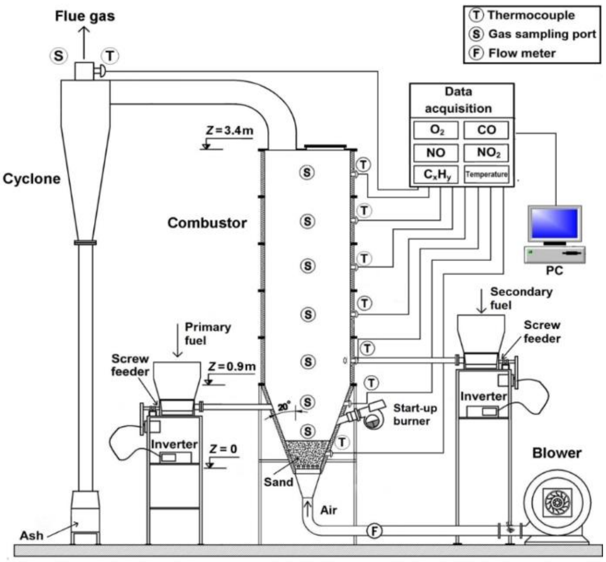

Figure 1. Schematic diagram of the experimental setup for fuel-staged co-firing of two biomass fuels.

2.2 The fuels and bed material

In co-combustion tests, pelletized rice husk (PRH) was used as the base (or primary) fuel, whereas moisturized rice husk (MRH) was injected downstream from the primary combustion zone as the secondary fuel.

PRH was supplied by a local company manufacturing pelletized biomass fuels. Prior to the pelleting process using a flat die fuel pellet machine, as-received rice husk was conveyed to a sieving system (to remove solid impurities) and then ground in a grinding mill to the specified particle size. Afterwards, the ground rice husk was fed together with some amount of water into the 100-hp pelletizer, which pressed the ground biomass into cylindrical pellets with a diameter of 6 mm and a variable length (between 5 and 15 mm). At the final stage, the pellets were spread onto a wire screen for cooling and drying, and, afterwards, were packed in fabric super sacks to keep up the fuel quality.

However, the secondary fuel was prepared by adding a specified amount of water to "as-received" rice husk supplied from a local rice mill. The average dimensions of MRH particles were 2-mm width, 0.5-mm thickness, and 10-mm length. Compared to burning "as-received" rice husk, the use of MRH with rather low calorific value prevented intensive formation of fuel-NO in the secondary combustion zone (mainly by low fuel-N content in MRH and reduced local temperature) and increased CO and C_xH_y levels, which enhances NO reduction reactions in this zone (Nussbaumer, 2003; Sirisomboon & Kuprianov, 2017).

Typically, rice husk contains about 40% C, 30% O, 5% H, up to 20% ash, and up to 10% moisture (all by weight, on as-received basis), whereas N and S contribute only small weight percentages (Fernandes *et al.*, 2016; Kuprianov *et al.*, 2011; Wannapeera *et al.*, 2008). However, during fuel processing (pelletizing and moisturizing), the fuel properties are subject to significant changes.

Table 1 presents the proximate and ultimate analyses, and the lower heating value of PRH and MRH (all presented on an "as-fired" basis) used in co-combustion experiments. From Table 1, the two types of rice husk had substantial contents of volatile matter making them highly reactive. Due to the higher moisture content in MRH, the lower heating value of this secondary fuel, LHV_{f2} = 10.6 MJ/kg, was noticeably lower than that of PRH, LHV_{f1} = 15.1 MJ/kg. It can be concluded that with its higher content of volatiles and high calorific value, PRH burned in the primary combustion zone (in effect, in the fluidized bed) and was more reactive than the MRH injected over the fluidized bed. Because of the insignificant S contents of both fuels, this work disregarded all issues related to formation and emission of SO_2 during co-firing of the selected fuels.

Silica sand (SiO_2 ≈ 88 wt.%), with 0.3–0.5 mm particle size and solid density of 2500 kg/m^3, was used as the bed material in this combustor when co-firing PRH and MRH. In all experiments the bed height was 30 cm (in a static state).

Table 1. Ultimate and proximate analyses, and the lower heating value (all on an as-fired basis) of the selected fuels used in (co-)combustion experiments.

Bio-mass	Ultimate analysis (wt.%)					Proximate analysis (wt.%)				LHV (kJ/kg)
	C	H	O	N	S	W	VM	FC	A	
PRH	43.27	5.04	31.17	0.79	0.02	9.81	64.9	15.39	9.90	15,100
MRH	29.94	3.01	22.93	0.34	0.01	29.56	41.9	14.33	14.21	10,600

2.3 Experimental methods for co-firing tests

In this work, the energy fraction of secondary fuel (EF_2) and the excess air (EA) were selected as independent operating parameters, while the total heat input to the reactor was constant (~200 kW_{th}) across all the experimental tests. To ensure this heat input, PRH and MRH were delivered into the reactor at respective mass flow rates ($\dot{m}_{f1}$ and $\dot{m}_{f2}$) for each (fixed) EF_2, quantified as the ratio of energy contribution by MRH ($\dot{m}_{f2}$ LHV_{f2}) to the total heat input to the combustor by both fuels ($\dot{m}_{f1}$ LHV_{f1} + $\dot{m}_{f2}$ LHV_{f2}).

In the first stage of this study, PRH was co-fired with MRH at different values of EF_2 (0, 0.1, 0.15, 0.2, and 0.25) while maintaining excess air constant (~40%), with the aim to investigate the effects of fuel staging on formation and oxidation/reduction of major gaseous pollutants inside the conical FBC. During a test run at fixed operating parameters (EF_2 and EA), temperature, O_2, CO, C_xH_y (as CH_4), and NO were measured along the reactor axial distance on centerline, as well as at the cyclone gas exit, using a new model "Testo-350" gas analyzer.

To investigate the effects of the operating parameters on emissions and combustion efficiency of the conical FBC, another test series was performed for the selected range of EF_2 while EA was varied from 20% to 80% for each fuel option. In this experimental series, only CO, C_xH_y (as CH_4), and NO emission concentrations were measured along with O_2 at the cyclone gas exit.

In each individual test run (at fixed EF_2 and EA) of the two experimental series, the actual amount of EA was quantified according to Basu *et al.* (2000), by using O_2, CO, and C_xH_y (as CH_4) measured at the cyclone exit.

2.4 Heat losses and combustion efficiency of the conical FBC for the co-firing tests

For each co-firing test, the heat loss due to unburned carbon and that due to incomplete combustion in the combustor were predicted according to Basu *et al.* (2000) using the 'equivalent fuel' concept, whose properties were determined as a weighted average from the corresponding properties and mass fractions (as the weights) of PRH and MRH (Sirisomboon & Kuprianov, 2017).

The heat loss due to unburned carbon ($q_{uc,cf}$, % LHV_{cf}) was predicted by using the carbon content in particulate matter (PM) emitted from the combustor (C_{PM}, wt.%) and the properties of the 'equivalent fuel', such as ash content (A_{cf}, wt.%) and lower heating value (LHV_{cf}, kJ/kg), as:

$$q_{uc,cf} = \frac{32{,}866 C_{PM}}{(100 - C_{PM})} \frac{A_{cf}}{LHV_{cf}} \tag{1}$$

Afterwards, the heat loss due to incomplete combustion ($q_{uc,cf}$, % LHV_{cf}) was quantified based on the CO and C_xH_y (as CH_4) concentrations at stack (both in ppm, at 6% O_2 and on a dry gas basis) and by taking into account the volume of dry combustion products originated from the combustion of the 'equivalent fuel' ($V_{dg,cf}$), as well as the LHV_{cf} (kJ/kg) and the above-calculated $q_{uc,cf}$ (%LHV_{cf}), as:

$$q_{\mathrm{ic,cf}} = (126.4\mathrm{CO} + 358.2\mathrm{C_xH_y})_{@6\%\mathrm{O_2}} \cdot 10^{-4} V_{\mathrm{dg,cf}} \frac{(100 - q_{\mathrm{uc,cf}})}{\mathrm{LHV_{cf}}} \quad (2)$$

The combustion efficiency of the conical FBC (%$\mathrm{LHV_{cf}}$) was then quantified as:

$$\eta_{\mathrm{cf}} = 100 - (q_{\mathrm{uc,cf}} + q_{\mathrm{ic,cf}}) \quad (3)$$

3. Results and Discussion

3.1 Effects of fuel staging on the axial temperature and O_2 profiles in the reactor

Figure 2 depicts the major combustion characteristics − the axial distribution of temperature and O_2 − in the conical FBC (co-) fired with PRH and MRH in various proportions at constant excess air. It can be seen in Figure 2 that the energy fraction of the secondary fuel (MRH), or fuel biasing, had noticeable effects on profiles of both temperature and O_2 inside the combustor.

In each trial (at fixed EF_2), the axial temperature profile was fairly uniform, exhibiting, however, a slight positive gradient in the bottom region of the combustor and a negative gradient in its upper region. The positive gradient was likely due to the impacts from (i) combustion air injected through the air distributor and (ii) endothermic devolatilization of PRH (occurred in the vicinity of fuel injection), whereas the negative gradient was mainly caused by the heat loss through combustor walls. These two regions met above the air distributor level at location of the peak temperature inside the reactor.

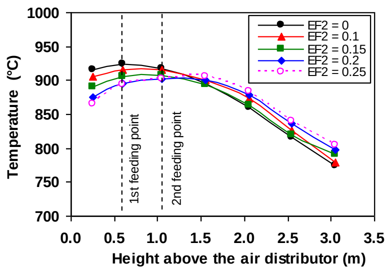

(a)

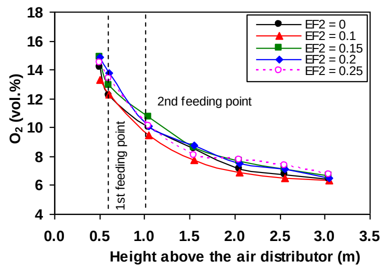

(b)

Figure 2. Effects of the energy fraction of secondary fuel (EF_2) on the axial profiles of (a) temperature and (b) O_2 in the conical FBC (co-)fired with PRH and MRH in different proportions at constant excess air (~ 40%).

From Figure 2a, with increasing EF_2 (at fixed EA), temperature at all points in the bottom region (including the peak temperature) was lower, mainly due to the reduced supply of the primary fuel (PRH), which increased the excess of air in this region. In the meantime, an increase of EF_2 from 0 to 0.25 shifted the peak temperature location from $Z = 0.6$ m (the level of PRH injection above the air distributor) to $Z = 1.6$ m, which was somewhat above the level of MRH injection.

It can be seen in Figure 2b that, in all the test runs, O_2 decreased along the reactor height, however with a weakening rate. A substantial axial gradient of O_2 was observed in the lower part of the reactor ($Z < 1.6$ m), comprising primary and secondary combustion zones, whereas in the upper part, the O_2 consumption (and, accordingly, fuel oxidation) along the combustor height occurred at an insignificant rate. However, unlike with temperature, O_2 did not show apparent effects from EF_2 in the fluidized-bed (bottom) region.

3.2 Formation and oxidation/reduction of gaseous pollutants in the conical FBC

Figure 3 shows the axial profiles of CO, C_xH_y (as CH_4), and NO in the conical FBC for the same operating parameters as in Figure 2. In all experiments, these profiles showed two specific regions (with an opposite behavior of the profiles) pointing at: (1) rapid (net) formation of the pollutants at the bottom part of the conical FBC and (2) highly-intensive secondary reactions in the reactor freeboard, such as oxidation of CO and C_xH_y, and reduction of NO. The shape of these profiles was mainly determined by the difference between the rate of primary (formation) processes/reactions and that of the secondary reactions in these two regions.

In the primary combustion zone (i.e., in effect, in the conical section with primary fuel injection), CO and C_xH_y originated from the fuel volatile matter and drastically increased along the combustor height, primarily due to the prompt devolatilization of PRH, followed/accompanied by oxidation of CO and C_xH_y, and fuel chars. While the CO oxidation occurred via its reactions with O_2 and OH, the C_xH_y oxidation reactions involved a breakdown of C_xH_y to CO, followed by oxidation of CO to CO_2 (Turns, 2006). It can be seen in Figure 3 (a and b) that in all the test runs, CO at different points inside the combustor was noticeably higher than C_xH_y, mainly due to the breakdown of C_xH_y to CO at high-temperature conditions.

At a rather low contribution of the secondary fuel (EF_2 = 0–0.15), the peaks of C_xH_y and CO were observed at the level of PRH injection ($Z \approx 0.6$ m), whereas at a greater heat input by MRH (EF_2 = 0.20–0.25), these peaks shifted to the secondary combustion zone (to the level of secondary fuel injection, $Z \approx 1.15$ m), as can be seen in Figure 3 (a and b). With increasing EF_2 within the specified range (at fixed EA of the reactor), the maximum values of CO and C_xH_y in the primary zone ($Z \approx 0.6$ m) decreased, mainly due to the reduced PRH feed rate and the corresponding increase (local) in excess air at this zone, which enhanced the oxidation of CO and C_xH_y in spite of the decreased bed temperature (Figure 2). However, CO and C_xH_y measured at $Z \approx 1.15$ m showed the opposite trend, generally due to the rapid devolatilization of MRH in the vicinity of its injection into the combustor.

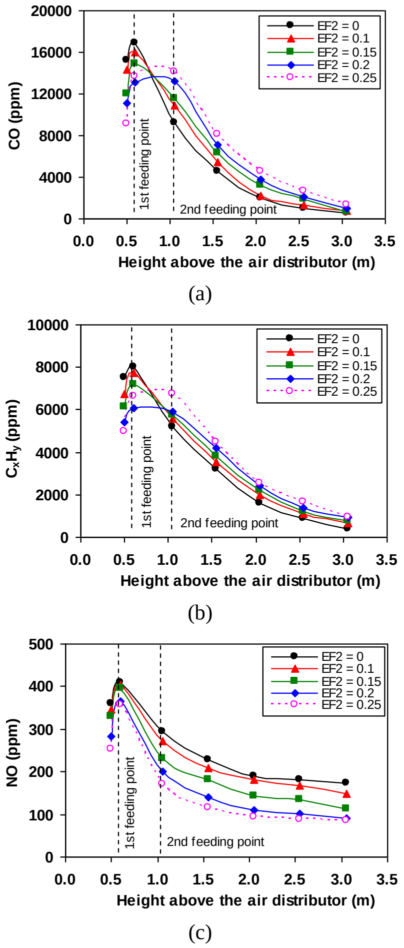

Figure 3. Effects of the energy fraction of secondary fuel (EF_2) on the axial profiles of (a) CO, (b) C_xH_y (as CH_4), and (c) NO in the conical FBC (co-) fired with PRH and MRH in different proportions at constant excess air (~ 40%).

With increasing EF_2 within the specified range (at fixed EA of the reactor), the maximum values of CO and C_xH_y in the primary zone ($Z \approx 0.6$ m) decreased, mainly due to the reduced PRH feed rate and the corresponding increase (local) in excess air at this zone, which enhanced the oxidation of CO and C_xH_y in spite of the decreased bed temperature (Figure 2). However, CO and C_xH_y measured at $Z \approx 1.15$ m showed the opposite trend, generally due to the rapid devolatilization of MRH in the vicinity of its injection into the combustor.

In the region above the secondary fuel injection, where the rate of the secondary (oxidation) reactions prevailed over the primary (formation) processes and reactions, both CO and C_xH_y gradually decreased along the reactor height to their minima (at the reactor top), showing the same effects from EF_2 as at $Z \approx 1.15$ m.

Like CO and C_xH_y, NO originated from the biomass volatile matter, via oxidation of volatile NH_3 and HCN by the numerous routes of the fuel-NO formation mechanism, including the proportional effects from fuel-N, excess air and temperature (Winter *et al.*, 1999; Werther *et al.*, 2000). However, due to some secondary reactions, such as heterogeneous reduction of NO by CO (mainly on the surface of fuel char particles) and homogeneous reactions of NO with light C_xH_y and NH_2/NH radicals, NO generated in the primary reactions was likely reduced to a substantial extent (Winter *et al.*, 1999; Werther *et al.*, 2000). It can be seen in Figure 3 (a and b) that the fuel staging extended the region with high concentrations of CO and C_xH_y, covering the secondary combustion zone, thus creating conditions for reducing a part of NO (formed during combustion of PRH in the bottom region) to N_2 in the secondary combustion zone.

Like with CO and C_xH_y, all axial NO profiles showed two specific regions in the combustor, as seen in Figure 3c. In the first (lower) region ($Z < 0.6$ m), where the rate of the NO formation reactions was significantly higher than that of the NO reduction reactions, NO increased rapidly along the combustor height, attaining the NO peak at $Z = 0.6$ m (at the level of primary fuel feeding) in all the test runs. With increasing EF_2, the NO peak at this point somewhat decreased, despite the increased excess air ratio at the primary combustion zone. This result can be likely attributed to the lowered bed temperature (Figure 2) and increased concentrations of CO and C_xH_y in this zone.

In the upper region of the axial NO profiles ($Z > 0.6$ m), the rate of the reactions responsible for NO reduction prevailed over NO formation, which led to a gradual decrease of NO along the reactor height. However, as seen in Figure 3c, with increasing EF_2, the NO reduction rate at $0.6 \text{ m} < Z < 1.5$ m was much higher than that at the combustor top, particularly at $EF_2 = 0.25$. This fact can be explained by the highest concentrations of both CO and C_xH_y in the vicinity of secondary fuel injection (when testing at the highest feeding of MRH), which enhanced the catalytic reduction of NO at the secondary combustion zone. Therefore, in the test at $EF_2 = 0.25$, NO at all points inside the combustor was at a minimal level, compared to the other tests.

3.3 Effects of operating parameters on the major gaseous emissions

Figure 4 depicts the CO, C_xH_y (as CH_4), and NO emissions from the conical FBC (all on a dry gas basis and at 6% O_2) when co-firing PRH and MRH at variable EF_2 and EA.

It can be seen in Figure 4 (a and b) that in all test runs with fuel staging, the CO and C_xH_y emissions from the combustor were increased compared to burning pure PRH. On increasing EA from about 20% to 40% (at fixed EF_2), these two emissions decreased significantly, showing however a rather weak effect of this operating parameter at its high values (60–80%). According to the domestic environmental legislation regarding biomass-fueled industrial applications (PCD, 2017), in order to meet the national emission limit for CO (740 ppm, as corrected to 6% O_2 on a dry gas basis), PRH and MRH should be co-fired at EF_2 not higher than 0.2 and EA = 40–80%.

In contrast, at fixed EA the fuel staging (via injecting MRH downstream from the primary combustion zone) gave lower NO emissions than individual burning of PRH (delivered through the lower fuel pipe), and the NO emission reduction became more significant as EF_2 was increased. This result can be generally attributed to the increased CO and

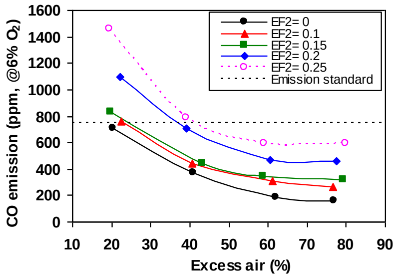

(a)

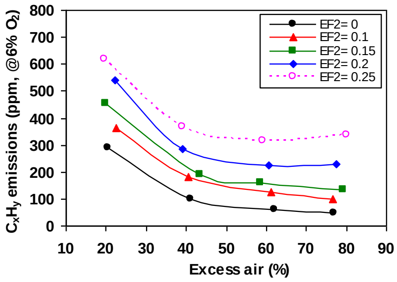

(b)

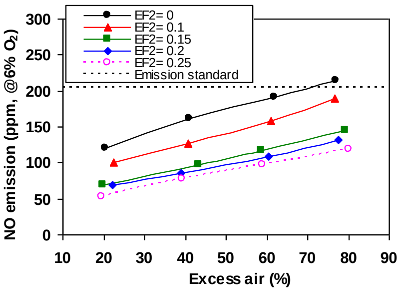

(c)

Figure 4. Emissions of (a) CO, (b) C_xH_y (as CH_4), and (c) NO from the conical FBC (co-)fired with PRH and MRH in different proportions at various air excess levels.

C_xH_y in the secondary combustion zone, which enhanced the catalytic reduction of NO in this zone. However, with increasing EA (for each fuel option), the NO emission was observed to increase, following the fuel-NO formation mechanism.

Note that, in all the tests with fuel staging, the NO emission was noticeably below the national emission limit for this pollutant (205 ppm, as corrected to 6% O_2 on a dry gas basis), as regulated by PCD (2017).

Figure 5 shows the NO emission reduction, as a function of EF_2 and EA. It can be seen in Figure 5 that this index was substantially affected by EF_2 but exhibited a weak effect from EA. At EF_2 = 0.1, the reduction efficiency was rather low, 12–22%, for the specified range of EA. However, as seen in Figure 5, the NO emission reduction can be increased to about 40% by switching EF_2 to 0.2–0.25 (regardless of EA).

Thus, fuel-staged co-firing of PRH and MRH with bottom air injection shows an apparent potential to reduce the NO emission from the conical FBC despite the elevated O_2 levels in the primary combustion zone.

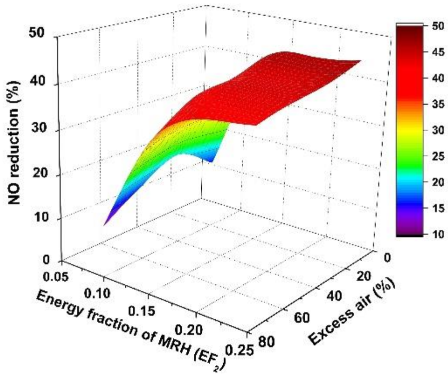

Figure 5. Effects of the energy fraction of secondary fuel (EF_2) and excess air on the NO emission reduction of the conical FBC when using fuel staging, relative to baseline use of only the primary fuel.

3.4 Heat losses and combustion efficiency of the conical FBC in test runs

Table 2 presents the predicted heat loss due to unburned carbon and that due to incomplete combustion together with the combustion efficiency of the proposed combustion technique co-fired with PRH and MRH at actual EF_2 and EA (or O_2 at stack). Some supporting variables required in Equations (1)–(3), such as the content of unburned carbon in PM and the CO and C_xH_y emission concentrations, are included in Table 2 as well.

As seen in Table 2, the two heat losses had important effects on the combustion efficiency of the conical FBC. When firing pure PRH (EF_2 = 0), the unburned carbon content in PM decreased from 3.63% to 1.98% as EA was increased from 21% to 77%, thus pointing at an increased rate of the char-C burnout with higher airflow rate. When using fuel staging, the impact of EA on unburned carbon in PM was minor. At EF_2 = 0.1–0.25, the carbon content in PM changed insignificantly when varying EA.

However, the CO and C_xH_y emissions, and consequently, the heat loss due to incomplete combustion showed quite strong influences of both EF_2 and EA. With increasing EA within the range (at any fixed EF_2), this heat loss decreased substantially. This result was generally due to the enhanced rates of CO and C_xH_y oxidation reactions. In contrast, with increasing EF_2 (at fixed EA), the heat loss due to incomplete combustion somewhat increased, which slightly reduced the combustion efficiency.

3.5 Operating conditions recommended for fuel-staged co-firing PRH and MRH

To reduce the environmental impact of NO emission, a more harmful pollutant than CO and C_xH_y, it is suggested that, at a fixed energy fraction of secondary fuel (EF_2), the excess air (EA) in the combustor be controlled to its least possible value, controlling however the CO emission to a level somewhat below the national limit for this pollutant. Based on this approach and aiming at the maximum reduction in NO emission, $EF_2 \approx 0.2$ and EA ≈ 40% can be regarded as the best option for the operating parameters when co-firing PRH and MRH in the conical FBC using fuel staging.

Table 2. Heat losses and combustion efficiency in the conical FBC when co-firing PRH and MRH at various combinations of EF_2 and EA.

Excess air (%)	O_2 at the cyclone exit (vol.%)	Unburned carbon in PM (wt.%)	CO[a] (ppm)	C_xH_y[a] (ppm)	Heat loss (%) due to: Unburned carbon	Heat loss (%) due to: Incomplete combustion	Combustion efficiency (%)
Individual firing of PRH (EF_2 = 0)							
21	3.7	3.63	709	290	0.81	0.74	98.4
41	6.2	3.15	373	98	0.70	0.31	99.0
62	8.1	2.09	184	61	0.46	0.17	99.4
77	9.1	1.98	158	46	0.44	0.14	99.4
Co-firing of PRH and MRH at EF_2 = 0.1							
22	4.0	1.47	759	364	0.36	0.86	98.8
41	6.1	2.89	440	180	0.71	0.45	98.8
61	8.0	3.02	311	125	0.74	0.32	98.9
77	9.1	2.89	265	101	0.71	0.26	99.0
Co-firing of PRH and MRH at EF_2 = 0.15							
20	3.7	2.12	835	455	0.54	1.03	98.4
43	6.4	2.49	440	192	0.64	0.48	98.9
59	7.8	2.51	347	160	0.64	0.39	99.0
79	9.3	2.30	317	134	0.59	0.34	99.1
Co-firing of PRH and MRH at EF_2 = 0.2							
22	4.0	2.93	1099	542	0.78	1.24	98.0
39	6.0	2.36	704	285	0.63	0.71	98.7
61	8.0	2.45	473	225	0.65	0.52	98.8
77	9.2	2.29	460	228	0.61	0.52	98.9
Co-firing of PRH and MRH at EF_2 = 0.25							
20	3.7	2.09	1463	618	0.58	1.51	97.9
39	6.0	1.96	783	368	0.54	0.86	98.6
59	7.9	2.13	595	317	0.59	0.70	98.7
80	9.4	2.33	593	337	0.65	0.73	98.6

[a]At 6% O_2 on dry gas basis

Under these conditions, an NO emission reduction by about 40% can be achieved from that with individual firing of the base fuel (PRH), while operating the combustor with quite high (~99%) combustion efficiency and controlling the CO emission within the national emission limit.

4. Conclusions

The effects of fuel staging on the emissions and combustion efficiency of a conical fluidized-bed combustor co-fired with pelletized rice husk (primary fuel) and moisturized rice husk (secondary fuel) have been investigated across a range of energy fractions of moisturized rice husk (in the total fuel supply) and a range of excess air. These two operating parameters have substantial effects on the formation and the oxidation/reduction of the major gaseous pollutants (CO, C_xH_y, and NO) in the primary and secondary combustion zones, as well as in the freeboard, and, consequently, on the emissions and combustion efficiency of the proposed combustion technique. With increasing the energy contribution of the secondary fuel to the reactor heat input and/or on lowering excess air, CO and C_xH_y in the secondary combustion zone increase, thus facilitating a noticeable decrease in NO in this zone and lowering the NO emission from this combustor using fuel staging with bottom air injection. The proposed co-firing method may insignificantly deteriorate the combustion efficiency. However, the co-firing of rice husk pellets and moisturized rice husk at 20% energy contribution by the secondary fuel (to the reactor heat input) and with about 40% excess air can ensure ~99% combustion efficiency and result in NO emission reduction by 60% from that when burning pelletized rice husk on its own.

Acknowledgements

The authors gratefully acknowledge the National Research Council of Thailand (NRCT), Phetchaburi Rajabhat University, as well as Thammasat University for supporting this research.

References

Areeprasert, C., Scala, F., Coppola, A., Urciuolo, M., Chirone, R., Chanyavanich, P., & Yoshikawa, K. (2016). Fluidized bed co-combustion of hydrothermally treated paper sludge with two coals of different rank. *Fuel Processing Technology*, *144*, 230–238. doi:10.1016/j.fuproc.2015.12.033

Basu, P., Cen, K. F., & Jestin, L. (2000). *Boilers and burners*. New York, NY: Springer.

Baukal, C. E. Jr. (2001). *The john zink combustion handbook*. New York, NY: CRC Press.

Chakritthakul, S., & Kuprianov, V. I. (2011). Co-firing of eucalyptus bark and rubberwood sawdust in a swirling fluidized-bed combustor using an axial flow swirler. *Bioresource Technology, 102*(17). 8268–8278. doi:10.1016/j.biortech.2011.06.056

Chyang, C. S., Qian, F. P., Lin, Y. C., & Yang, S. H. (2008). NO and N_2O emission characteristics from a pilot scale vortexing fluidized bed combustor firing different fuels. *Energy and Fuels, 22*(2). 1004–1011. doi:10.1021/ef7005595

Department of Alternative Energy Development and Efficiency, Ministry of Energy, Thailand. (2014). *Thailand alternative energy situation 2014*. Retrieved from http://www.dede.go.th/download/state_58/sit_57_58/Thailand%20Alternative%20Energy%20Situation.pdf

Duan, F., Chyang, C. S., Lin, C. W., & Tso, J. (2013). Experimental study on rice husk combustion in a vortexing fluidized-bed with flue gas recirculation (FGR). *Bioresource Technology, 134*, 204–211. doi:10.1016/j.biortech.2013.01.125

Fang, M., Yang, L., Chen, G., Shi, Z., Luo, Z., & Cen, K. (2004). Experimental study on rice husk combustion in a circulating fluidized bed. *Fuel Processing Technology, 85*(11), 1273–1282. doi:10.1016/j.fuproc.2003.08.002

Fernandes, I. J., Calheiro, D., Kieling, A. G., Moraes, C. A. M., Rocha, T. L. A. C., Brehm, F. A., & Modolo, R. C. E. (2016). Characterization of rice husk ash produced using different biomass combustion techniques for energy. *Fuel, 165*, 351–359. doi:10.1016/j.fuel.2015.10.086

Janvijitsakul, K., & Kuprianov, V. I. (2008). Major gaseous and PAH emissions from a fluidized-bed combustor firing rice husk with high combustion efficiency. *Fuel Processing Technology, 89*(8), 777–787. doi:10.1016/j.fuproc.2008.01.013

Kuprianov, V. I., Janvijitsakul, K., & Permchart, W. (2006). Co-firing of sugar cane bagasse with rice husk in a conical fluidized-bed combustor. *Fuel, 85*(4), 434–442. doi:10.1016/j.fuel.2005.08.013

Kuprianov, V. I., Kaewklum, R., & Chakritthakul, S. (2011). Effects of operating conditions and fuel properties on emission performance and combustion efficiency of a swirling fluidized-bed combustor fired with a biomass fuel. *Energy, 36*(4), 2038–2048. doi:10.1016/j.energy.2010.05.026

Kuprianov, V. I., Kaewklum, R., Sirisomboon, K., Arromdee, P., & Chakritthakul, S. (2010). Combustion and emission characteristics of a swirling fluidized-bed combustor burning moisturized rice husk. *Applied Energy, 87*(9), 2899–2906. doi:10.1016/j.apenergy.2009.09.009

Madhiyanon, T., Lapirattanakun, A., Sathitruangsak, P., & Soponronnarit, S. (2006). A novel cyclonic fluidized-bed combustor (ψ-FBC): Combustion and thermal efficiency, temperature distributions, combustion intensity, and emission of pollutants. *Combustion and Flame, 146*(1–2), 232–245. doi:10.1016/j.combustflame.2006.03.008

Madhiyanon, T., Piriyarungroj, N., & Soponronnarit, S. (2004). A novel vortex-fluidized bed combustor with two combustion chambers for rice-husk fuel. *Songklanakarin Journal of Science and Technology, 26*(6), 875–893.

Madhiyanon, T., Sathitruangsak, P., & Soponronnarit, S. (2010). Combustion characteristics of rice-husk in a short-combustion-chamber fluidized-bed combustor (SFBC). *Applied Thermal Engineering, 30*(4), 347–353. doi:10.1016/j.applthermaleng.2009.09.014

Narayanan, K. V., & Natarajan, E. (2007). Experimental studies on cofiring of coal and biomass blends in India. *Renewable Energy, 32*(15), 2548–2558. doi:10.1016/j.renene.2006.12.018

Ninduangdee, P., & Kuprianov, V. I. (2015). Combustion of an oil palm residue with elevated potassium content in a fluidized-bed combustor using alternative bed materials for preventing bed agglomeration. *Bioresource Technology, 182*, 272–281. doi:10.1016/j.biortech.2015.01.128

Ninduangdee, P., & Kuprianov, V. I. (2016). A study on combustion of oil palm empty fruit bunch in a fluidized bed using alternative bed materials: Performance, emissions, and time-domain changes in the bed condition. *Applied Energy, 176*, 34–48. doi:10.1016/j.apenergy.2016.05.063

Nussbaumer, T. (2003). Combustion and co-combustion of biomass: Fundamentals, technologies, and primary measures for emission reduction. *Energy and Fuels, 17*(6), 1510–1521. doi:10.1021/ef030031q

Pollution Control Department, Ministry of Natural Resources and Environment, Thailand. (2017). *Air pollution standards for industrial sources*. Retrieved from http://www.pcd.go.th/info_serv/reg_std_airsnd03.html

Sahu, S. G., Chakraborty, N., & Sarkar, P. (2014). Coal–biomass co-combustion: An overview. *Renewable and Sustainable Energy Reviews, 39*, 575–586. doi:10.1016/j.rser.2014.07.106

Salzmann, R., & Nussbaumer, T. (2001). Fuel staging for NO_x reduction in biomass combustion: Experiments and modeling. *Energy and Fuels, 15*(3), 575–582. doi:10.1021/ef0001383

Sami, M., Annamalai, K., & Wooldridge, M. (2001). Co-firing of coal and biomass fuel blends. *Progress in Energy and Combustion Science, 27*(2), 171–214. doi:10.1016/S0360-1285(00)00020-4

Sirisomboon, K., & Kuprianov, V. I. (2017). Effects of fuel staging on the NO emission reduction during biomass–biomass co-combustion in a fluidized-bed combustor. *Energy and Fuels, 31*(1) 659–671. doi:10.1021/acs.energyfuels.6b02622

Turns, S. (2006). *An introduction to combustion*. Boston, MA: McGraw-Hill.

Visser, H. J. M., Van Lith, S. C., & Kiel, J. H. A. (2008). Biomass ash-bed material interactions leading to agglomeration in FBC. *Journal of Energy Resources Technology, Transactions of the ASME, 130*(1), No. 0118011–0118015. doi:10.1115/1.2824247

Wannapeera, J., Worasuwannarak, N., & Pipatmanomai, S. (2008). Product yields and characteristics of rice husk, rice straw and corncob during fast pyrolysis in a drop-tube/ fixed-bed reactor. *Songklanakarin Journal of Science and Technology, 30*(3), 393–404.

Werther, J., Saenger, M., Hartge, E. U., Ogada, T., & Siagi, Z. (2000). Combustion of agricultural residues. *Progress in Energy and Combustion Science, 26*(1), 1–27. doi:10.1016/S0360-1285(99)00005-2

Winter, F., Wartha, C., & Hofbauer, H. (1999). NO and N_2O formation during the combustion of wood, straw, malt waste and peat. *Bioresource Technology, 70*(1), 39–49. doi:10.1016/S0960-8524(99)00019-X